SSRG International Journal of Electronics and Communication Engineering
ISSN: 2348-8549/ https://doi.org/10.14445/23488549/IJECE-V11I8P128

Volume 11 Issue 8, 294-300, August 2024
© 2024 Seventh Sense Research Group®

Original Article

STC Using Coastal Map and Wavelet Transform for Sea Clutter Suppression

R. Navya[1], Devaraju Ramakrishna[2], Sneha Sharma[3]

[1]*Department of ECE, Dayananda Sagar University, Karnataka, India.*
[2]*Department of ETE, Dayananda Sagar College of Engineering, Karnataka, India.*
[3]*Department of ECE, Dayananda Sagar University, Karnataka, India.*

[1]*Corresponding Author : navya-ece@dsu.edu.in*

Received: 22 June 2024 Revised: 01 August 2024 Accepted: 16 August 2024 Published: 31 August 2024

Abstract *- Detecting small or low-visibility targets in the presence of rough sea clutter is a critical challenge in coastal radar systems. Sea clutter refers to the unwanted echoes or reflections of radar signals caused by the dynamic sea surface majorly due to wind, waves, and other environmental factors. These echoes can mask the Radar returns from smaller targets like boats or aircraft, particularly at closer ranges. The complex and dynamic nature of this sea clutter poses a considerable challenge in the detection of targets of interest. The detection and tracking of targets of interest in marine situations are effectively improved by suppressing sea clutter. Sensitivity Time Control (STC) is a powerful method for mitigating near-range sea clutter, leveraging both spatial and temporal characteristics of the clutter returns. The STC curve estimate technique reduces the strength of signals from nearby range bins and marine clutter. STC curve estimation begins from the Radar transmit cover pulse on the received radar data. Attenuation is kept to the maximum during the on time transmit cover pulse. Rather than beginning curve estimation at the real coastal point (or range offset), the third order STC estimation using the raw input data for the mitigation of the sea clutter is approximated from the radar location for all the azimuth change pulse (ACP). Because of this, the calculated curve cannot adequately capture the abrupt transients at the land-water contact. Hence, a method is proposed for near range clutter mitigation using geographic map sources, like Global Self Consistent Hierarchical High Resolution Geographical (GSHHG) maps for finding coastal intersection points and Wavelet Transforms for finding erroneous sharp peaks.*

Keywords *- STC, GSHHG, Radar data, ACP, Clutter.*

1. Introduction

Target detection and tracking is a critical step in ensuring the safety and security of the coastal environment. The primary goal of the radar system is to detect and track objects of interest, such as ships, small boats, buoys and low-flying aircraft. The majority of radar reflections come from land and marine areas. Radar waves could be reflected off of land, terrain, flora, man-made structures, vessels, and other objects. In general, echoes from the land and dynamic sea surface, etc., are typically regarded as undesired reflections or clutter because they obscure reflections from targets of interest, such as small boats and ships. Since waves, tides, and other external variables affect sea clutter, clutter characteristics are more dynamic. Its dynamic nature necessitates adaptive detection approaches since it might cause short-term shifts in the characteristics of the clutter. Therefore, a significant issue in radar data processing is separating actual targets from common false targets or clutters. Sensitivity Time Control (STC) is one of the several clutter reduction strategies [1] used by radar surveillance systems to reduce near-range interference from the land and rough water surface.

Sensitivity Time Control (STC) is a technique used in coastal radar systems to control the radar receiver's sensitivity over time following a transmission pulse. The main purpose of STC is to mitigate the undesired near range reflected signals, such as sea clutter or ground reflections. These undesired reflections are strongest near the Radar. They can also mask the presence of smaller or long-distance targets. At the moment when clutter is most likely to happen, right after the pulse is transmitted, STC lowers the receiver gain or maximizes the threshold. By gradually increasing the gain or decreasing the threshold, the STC enables the surveillance radar to detect weaker signals from long-distance targets. The output curve generated in the STC clutter suppression model is inversely proportional to the increase in Range(R) with reduction factor 'A' as shown in Figure 1. The STC curve must be calibrated correctly. Close-range targets may go undetected by the radar processor if the sensitivity is drastically lowered. On the other hand, clutter could still overwhelm the receiver and, in-turn, display if it is not reduced optimally. Gain control over time can be dynamically modified in response to current conditions or predefined in accordance with the particular operating environment.

This is an open access article under the CC BY-NC-ND license (http://creativecommons.org/licenses/by-nc-nd/4.0/)

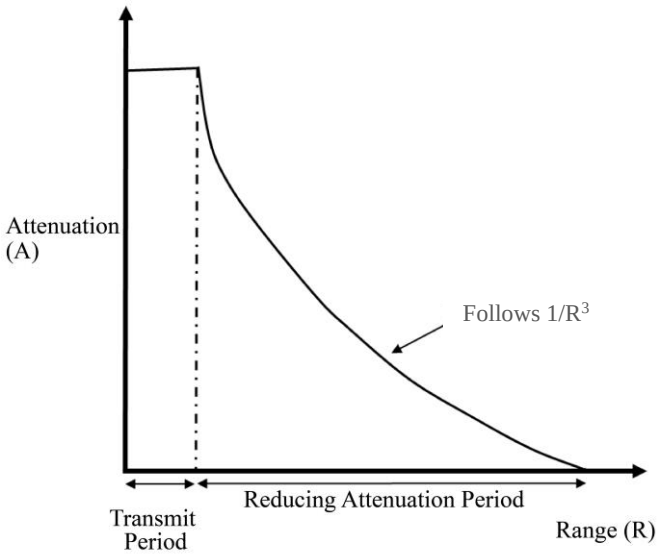

Fig. 1 Sensitivity time control

The crucial point is that the sea equivalent RCS is proportionate to R since the illuminated area is proportional to the range R. Unlike ordinary targets, the sea's RCS grows with distance. For rain, the variation in reduction of intensity over distance may be on the order of R^2, whereas for marine or ground clutter scenarios, it will be of the order R^3[2]. Typically, STC curve estimation begins from the Radar transmit cover pulse on the received raw intensity values.

Attenuation is kept to the maximum during the on time transmit cover pulse. Rather than beginning curve estimation at the real coastal intersection point, the third order STC estimation using the raw input data for the mitigation of the sea clutter is approximated from the radar location. Because of this, the calculated curve cannot adequately capture the abrupt transients at the land-water contact at the coastal border. Consequently, the output of the STC curve fitting [3-4] on the sensor data input will have undesired leftover of clutter signals distributed across all the azimuth at the near range of the Radar, which negatively impacts target detection and visual representation. By using GSHHG maps [13], coastal intersection points can be identified.

High-resolution, publicly available shoreline data was combined from two widely recognized database sources, World Vector Shorelines (WVS) and World Data Bank II (WDB), to create GSHHG Maps [1]. The complete GSHHG data set can be downloaded from the U.S. National Oceanic and Atmospheric Administration (NOAA). Rivers, lakes, political boundaries, and coastlines are all included in the WDBII database. Shorelines at land/ocean interfaces are found in WVS.Geography data are in five resolutions: crude, low, intermediate, high, and full. Shorelines are organized into four levels: boundary between land and ocean, boundary between lake and land, boundary between island-in-lake and lake and boundary between pond-in-island and island. GSHHG Maps aid in defining the coast and starting the estimate of the STC curve from coastal boundary points [13].

Erroneous peaks present in the near range reflections will contribute majorly to the curve estimation. The presence of these peaks may lead to a wrong estimation of the curve. Peaks with higher intensity may overestimate the curve, resulting in the masking of the target. Peak and valley point identification across all the azimuth angles can be accomplished using Wavelet Transform. The Continuous Wavelet Transform (CWT) is particularly useful for detecting peaks and valleys because it provides a continuous analysis of the signal across different scales. By observing the wavelet coefficients at different scales, the presence of peaks and valleys can be identified. A positive peak in the echoed signal normally corresponds to a large positive wavelet coefficient at finer scales. Finding peaks and valleys of different sizes is made easier by examining the signal at different scales. This is especially helpful for complex signals like reflections from varying sea surfaces, as features may occur at multiple scales.

The STC curve estimation might be constant throughout radar azimuth angular resolution beam width since, typically, it is assumed that the clutter model is isotropic [5]. But in real time scenarios, the radar reflections from the sea surface vary with each ACP due to varying sea conditions. Typical reflections from the sea surface and target for an ACP are shown in Figure 2.

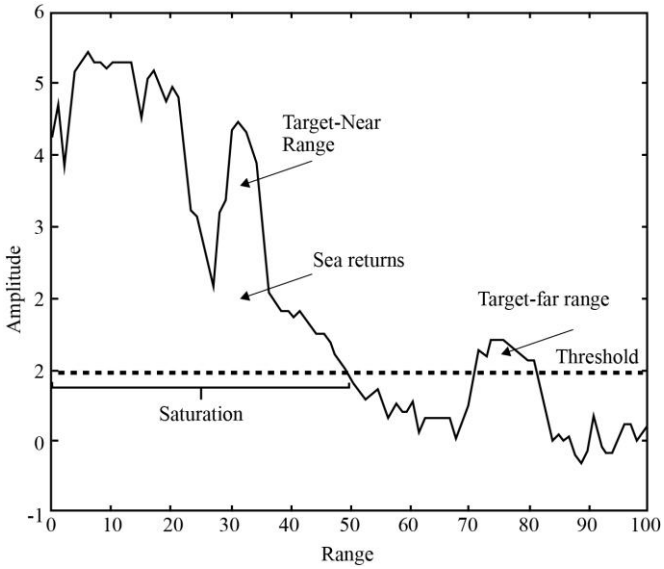

Fig. 2 Typical radar returns of an ACP

Each azimuth angle estimation should begin at the edge of the coastline region. Coastal boundary varies for each azimuth angle with respect to the radar location. Therefore, in comparison to a constant range offset for all angles, the GSHHG Map aids in the determination of these boundary locations and offers improved curve estimation. These coastal intersection points can also be used to mask the unwanted

reflections from the land. Complete masking of reflections from land reduces the number of unwanted detections and false tracks. Due to the reduction in false plots, the track load on the processing module will be reduced.

In this paper, a novel method is proposed for polynomial STC curve estimation from coastal intersection points using Wavelet Transforms and GSHHG maps. Intersection points of seawater with land are extracted for every ACP angle resolution. These points are used for STC curve estimation. Peaks along with the Valley points in the ACP are found using wavelet transform, which is removed before estimation of the curve.

2. Literature Survey

A. Parsa et al. [6] present the comparison of target detection in sea clutter and analysis of its performance with horizontally and vertically polarized radar antennas. The work analyses the target detection in the existence of rough sea clutter with 72% accuracy and interference-controlling strategies with an experimental setup. M. Martorella et al. [7] discuss the method to minimize the marine clutter effect on the target of interest using the fractal dimension of sea surface backscattered signal at low grazing angle.

Xianwen Ding et al. [2] explain how to suppress marine clutter, utilizing sensors intended for radar navigation to acquire a temporal series of radar pictures. These sensors mostly operate in the X-band and are utilized in coherent radars with horizontal polarization. It was suggested that the best way to minimize the impact of sea clutter on targets was to use time-based navigation image sequences for the CFAR approach.

Yong Yang et al. [8] introduce an Orthogonal Projection(OP) approach to suppress the sea clutter and combine OP with the Constant False Alarm Rate (CFAR) of Cell Averaging (CA). An experiment was carried out to demonstrate and compare the complexity of OP and clutter suppression averaging with Singular Value Decomposition (SVD).

Wei Jing et al. [9] provide a thorough analysis of a novel algorithm known as the Extreme Learning Machine [ELM] for target locating in the presence of sea clutter. The algorithm classifies the features of the sea clutter and analyzes it by taking into account its correlation characteristics, which are further separated into temporal and spatial correlation. It was ultimately determined that an extreme learning machine is capable of effectively separating the target in the presence of clutters from the sea returns.

According to a new approach proposed by W. Biamino et al., Sobel edge extraction is used to identify the edges of all objects from KOMPSAT-5 X-band SAR images. The edges of the land objects are then combined with the edges from the ENC coasts. Geometrically corrected SAR pictures were masked using the land mask data before a ship detection technique was applied. Thus, in coastal waters, this technique can help with accurate ship recognition utilizing SAR photos.

3. Proposed Polynomial Curve Fitting Method to Implement Sensitivity Time Control (STC)

The proposed method to suppress the near range clutter has been implemented in the following steps:

3.1. STC Curve Estimation

In general, for estimation of STC on return, clutter is typically assumed to be uniform throughout the radar's azimuth angle. Because it is assumed that the clutter model is isotropic, the STC estimation [2] [11] might be constant throughout radar azimuth angular resolution beam width. A non-isotropic clutter model is applied in real-time scenarios to improve the results of clutter suppression because the strength of the clutter fluctuates greatly with changes in azimuth angles. As a result, STC curve estimation is done at all radar angles.

By using wavelet transform, erroneous peaks are detected in the data set for each ACP. Locating an ACP's local maxima and minima is the process of peak detection. There are typically both high-frequency and low-frequency components in returned signals. It is necessary to have coarse time resolution but fine frequency resolution for low-frequency components because they fluctuate slowly over time. High-frequency components need coarse frequency resolution but high time resolution because they change quickly with time. As a result, when examining a signal that has both low- and high-frequency components, a multiresolution method of analysis is helpful.

The Continuous Wavelet Transform (CWT) of a signal x(t) with respect to a wavelet function ψ(t) is given by [10]

$$W_x\,(a, b) = \frac{1}{\sqrt{|a|}} \int_{-\infty}^{\infty} x(t)\Psi * \left(\frac{t-b}{a}\right) dt$$

Where ‘a’ and ‘b’ are the scale and translation parameters

Peaks and valleys are found in the wavelet transform coefficients following the acquisition of the CWT [12] coefficients W_x (a, b). Typically, valleys denote local minima, while peaks imply abrupt shifts or local maxima. Once Sharp peaks and sudden dips are found, intensity in these points is normalized with subsequent range bin intensity value before estimating the polynomial STC curve.

Polynomial STC curve estimate is a curve fitting method that approximates a curve over the provided "n" data points in order to capture the trend in the data. Fitting a k^{th} order polynomial with the available coefficients a_i., for the required “n” number of points (x_i, y_i) is given as [2] [16],

$$y = a_0 + a_1x + a_2x^2 + \cdots + a_kx^k$$

For the minimal residual values, curve fitting can be represented in Matrix format Xa = Y as below,

$$\begin{bmatrix} n & \sum_{i=1}^{n} x_i & \cdots & \sum_{i=1}^{n} x_i^k \\ \sum_{i=1}^{n} x_i & \sum_{i=1}^{n} x_i^2 & \cdots & \sum_{i=1}^{n} x_i^{k+1} \\ \vdots & & \ddots & \vdots \\ \sum_{i=1}^{n} x_i^k & \sum_{i=1}^{n} x_i^{k+1} & \cdots & \sum_{i=1}^{n} x_i^{2k} \end{bmatrix} \begin{bmatrix} a_0 \\ a_1 \\ \vdots \\ a_k \end{bmatrix} = \begin{bmatrix} \sum_{i=1}^{n} y_i \\ \sum_{i=1}^{n} x_i y_i \\ \vdots \\ \sum_{i=1}^{n} x_i^k y_i \end{bmatrix}$$

Here, "X" represents the Vandermonde matrix. With an equation such as $a = X^{-1}Y$, the resultant vector 'a' can be calculated. For the polynomial curve estimation of the input data, matrix 'X' is the value of the range resolution cell set. Equivalent intensity values for the same range resolution and Azimuth resolution cell are used in matrix 'Y'.

3.2. Finding Coastal Intersection Points

The boundaries of land and sea can be found for each minimal azimuth angle by utilizing the coastal map. The GSHHG map data was obtained from the official source. The GSHHG dataset is available from NOAA [13]. It is available in a variety of formats, including shapefiles and binary formats.

A map of roughly 150 km is downloaded from the radar location. Radar position is found using GPS, which gives the latitude and longitude information of the radar location. Data is available in five resolution levels. High resolution is chosen to find the coastal intersection points.

Downloaded map files are extracted and analyzed using the Mat Lab 'Mapping toolbox'. Libraries are used to decompress and unzip the data file. Scrutinize the extracted data set to select the required level of data. Overlay the extracted shoreline points with raw data using open-source GIS software QGIS. Visualize the intersection points on a map within the Geographic Information System (GIS) software to verify correctness.

Any discrepancy between the map and the presentation could be caused by a variety of factors, including dynamic changes in sea level, recently constructed man-made structures, changes in geography brought on by natural disasters, inaccurate representations of map data, inaccurate radar beam widths, etc. Coastal points can be adjusted as per the observation to cater for any misalignment of the shoreline with a presentation on GIS display.

Since the STC Curve represents an estimate of the sea clutter [14] [16], the intensity value of the STC curve is deducted from the corresponding real-time radar sensor data. Optimal estimation of the STC curve will result in lesser residual of the returned signals.

A functional flow diagram is explained in Figure 3. First, coastal intersection points are extracted using the Mat Lab functions. These land and sea intersection points are stored for each Azimuth angle. The unprocessed raw data set is processed to remove sharp peaks using wavelet transform. After this stage, using the coastal intersection points, the STC curve [15] is estimated only on the sea portion. Estimation is done for all ACPs independently. Finally, intensity values of the estimated curve are detected from the original unprocessed raw intensity of the same corresponding data points.

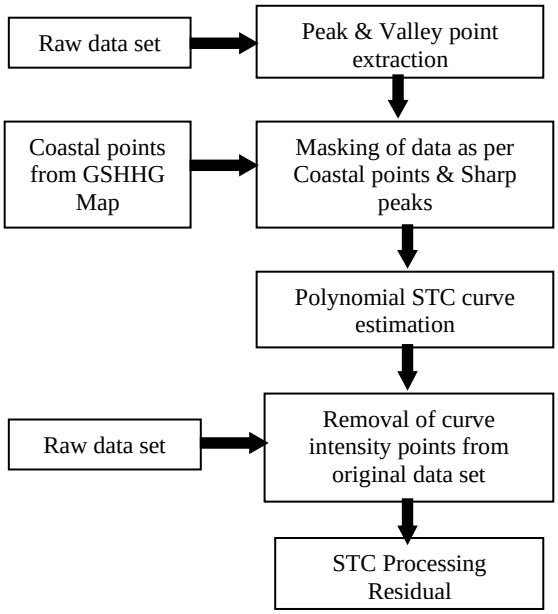

Fig. 3 Processing flow diagram of STC

4. Results and Discussion

The proposed scheme of near range clutter mitigation is applied to the sensor data set, which is captured by fixing the radar location on the coastline.

The coastal map is extracted, and land water intersection points are calculated using Mat Lab functions. Intersection points can be readjusted by mapping land and sea surfaces with the geographical map of the Radar installed location using a GIS display.

Google map and GSHHG map for the radar location are shown in Figure 4. Label 'A' and 'B' denote the points of association between the two images. Returns from the land are denoted by 'A', and 'B' represents the returns from the sea. The coastline limit from where the polynomial STC curve computation should start is indicated on the map. Every azimuth angle has its own set of coastline spots calculated.

(a)

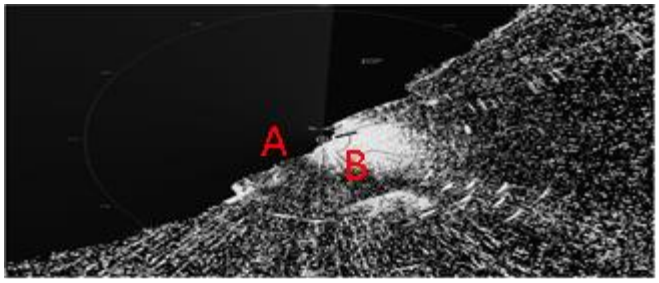

(b)

Fig. 4(a) Coastal area google map (b) The same geographic shown using the GSHHG map

As shown in Figure 4(b), strong near range reflections from varying sea conditions can saturate the receiver and in-turn display. One full scan data set is presented on the GIS display, as shown in Figure 5. It displays the unprocessed raw data, which is loaded for about a 100 km radius from the radar installation location. Strong reflections from the land portion are predominantly present on the display, which may lead to false target detection and tracking. As shown in Figure 5(b), using the GSHHG map, land returns from the land portion are completely masked.

This resulted in reduced processing load as well as the reduction in fall detection and tracking of unwanted clutter as the target. The STC curve is estimated for each azimuth angle on the data from sea reflection [8]. Display saturation happens when the Radar receives signals that are so strong that they overpower the display, making it challenging to distinguish between various return types. This frequently manifests as big, bright patches on a radar screen that obstruct or distort the image of other objects. Strong signals may overpower the screen due to saturation, potentially hiding the existence of smaller or weaker targets and creating a cluttered radar display.

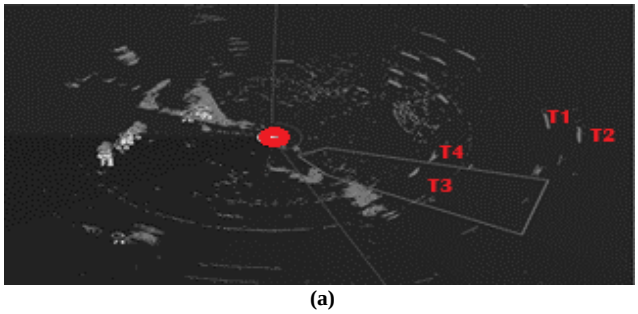

(a)

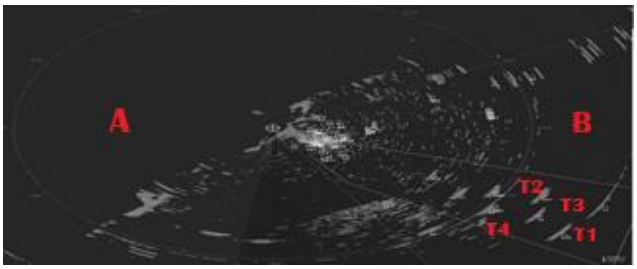

(b)

Fig. 5 (a) Raw data of full 360^0 azimuth coverage (b) Land masked raw data

In Figure 6, The input signal raw data intensity for an azimuth count pulse at a 90-degree angle is represented by the red color curve. The black colored line represents the estimated polynomial STC Curve. The residue is represented using blue color. There is a denser residue in the range cells, which are nearer to the Radar because the third order STC estimation on the raw input data is approximated from the transmit cover pulse of the Radar, as in Figure 6(a). Figure 6(b) represents polynomial curve estimation using coastal intersection points. Using wavelet transform, local maxima and minima are found and removed before the curve is estimated from the input data. The residual plot is represented in blue color. Since the estimation of the curve is started from the coastal point, the land portion is masked, and no residue is left till the coast. The curve is not erroneous due to the removal of local maxima from the input data.

A distinct land body is identified for each segment of an azimuth count pulse if there are several coastline locations present, as shown in Figure 7. Without taking into account intermediate breakpoints, a single STC curve is predicted for the whole data set in an azimuth count pulse and displayed as a black colored line, as shown in Figure 7(a). The computation of residue is done by considering the intermediate land patches using map points, as shown in Figure 7(b).

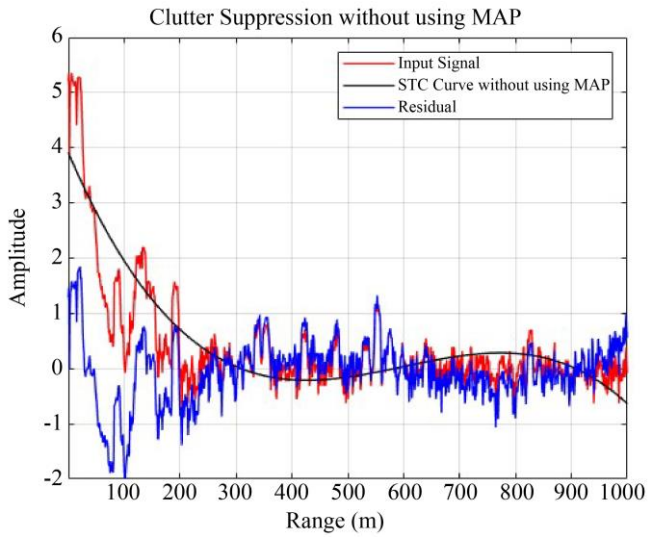

(a)

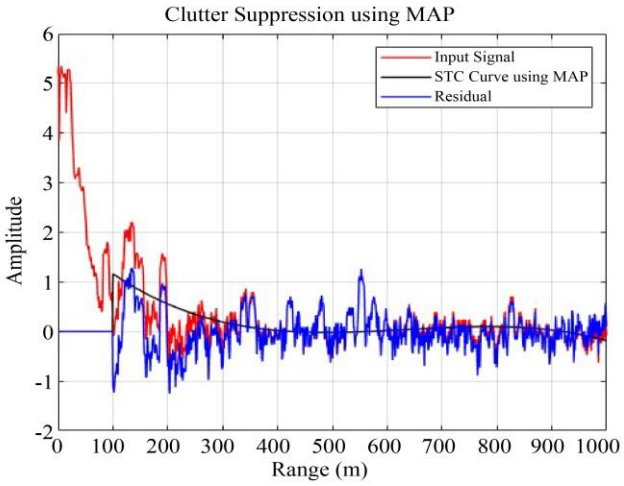

(b)

Fig. 6 Near range clutter suppression (a) Suppression from radar location (b) Suppression from coastal boundary using map

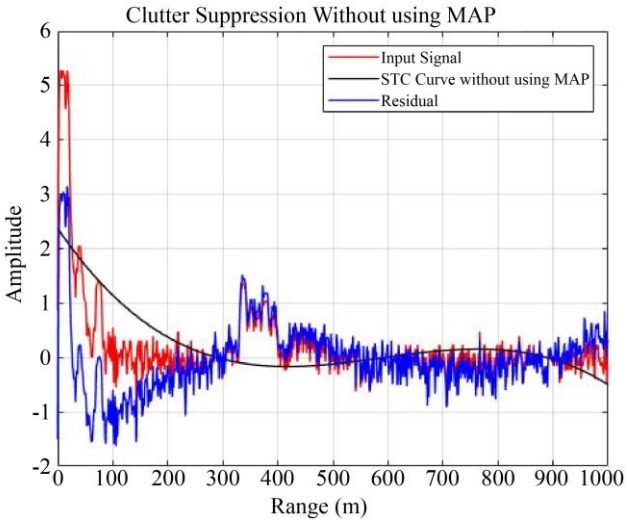

(a)

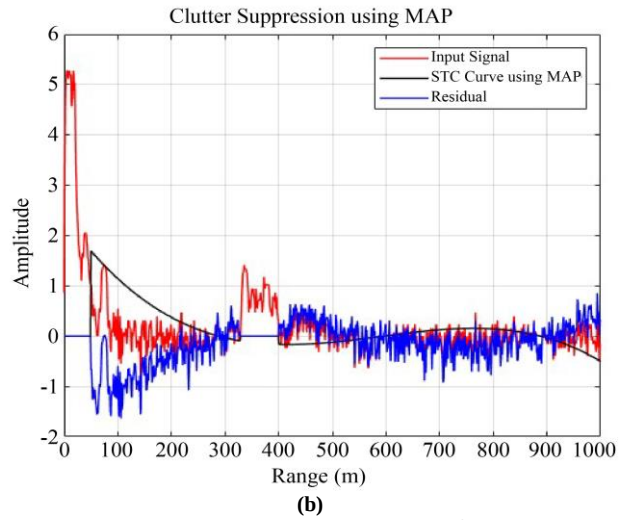

(b)

Fig. 7 STC-based clutter mitigation (a) Suppression from radar location up to full range(b) Mitigation by masking intermediate land patch using the map

Sharp peaks present in the data set are shown in Figure 8. Without removing the sharp peaks in the input data set, the STC curve is predicted for the whole data set in an azimuth count pulse and displayed as a black colored line, as shown in Figure 8(a). Using wavelet transform, sharp peaks are identified and removed before the estimation of STC, as shown in Figure 8(b).

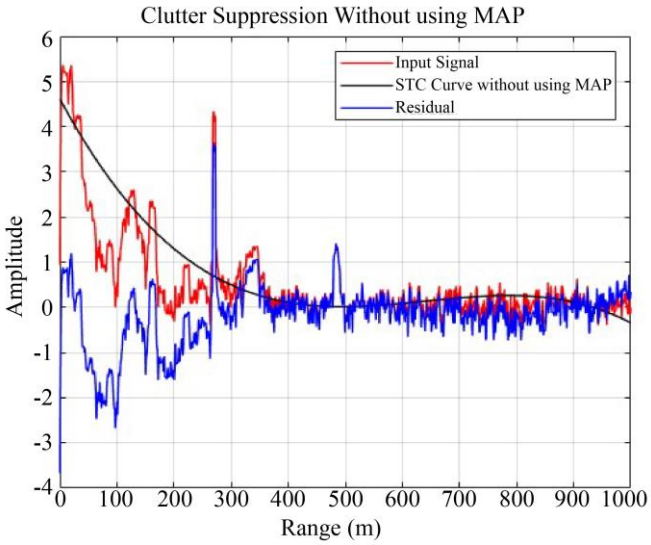

(a)

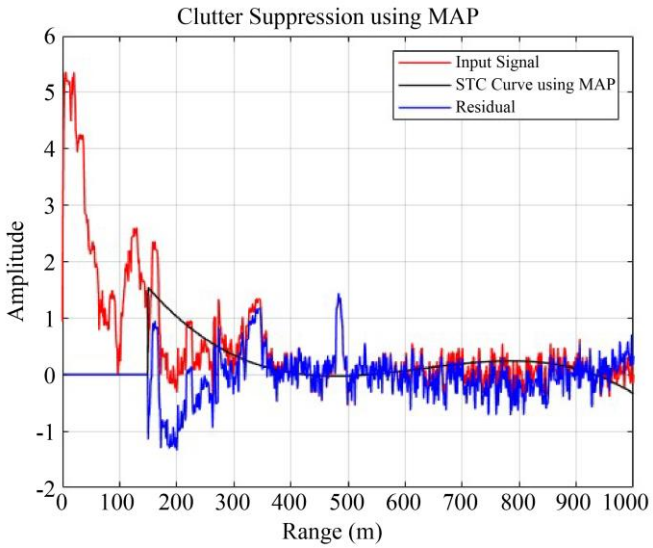

(b)

Fig. 8 STC-based clutter mitigation (a) Suppression from radar location (b) Suppression from coastal boundary using the map and by eliminating sharp peak

5. Conclusion

Polynomial curve fitting based STC is implemented using a GSHHG map and Wavelet Transform. When compared to the conventional STC method, map-based and Wavelet transform-based polynomial STC offers superior clutter suppression inner ranges. Map points aided in masking unwanted echo from the land region

completely, which improved the better display visibility and proceeding load. The discrepancy between the map and the data is due to the dynamic changes in sea level. Recently constructed man-made structures have been readjusted using GIS software. Sharp peaks and valleys are found using wavelet transform, which helped in the exact estimation of the curve for each azimuth angle.

References

[1] Thomas E Wood, "*Methods and Apparatus for Automatic STC from Sea State Measurement via Radar Sea Clutter Eccentricity*," US8456352B2, 2013. [Google Scholar]

[2] Xianwen Ding et al., "Ship Detection in Presence of Sea Clutter from Temporal Sequences of Navigation Radar Images," *MIPPR 2009: Automatic Target Recognition and Image Analysis*, vol. 7495, 2009. [CrossRef] [Google Scholar] [Publisher Link]

[3] Wenjing Zhao, Zhe Chen, and Minglu Jin, "Subband Maximum Eigenvalue Detection for Radar Moving Target in Sea Clutter," *IEEE Geoscience and Remote Sensing Letters*, vol. 18, no. 2, pp. 281-285, 2020. [CrossRef] [Google Scholar] [Publisher Link]

[4] W. Biamino et al., "A "Dynamic" Land Masking Algorithm for Synthetic Aperture Radar Images," *2015 IEEE International Geoscience and Remote Sensing Symposium (IGARSS)*, Milan, Italy, pp. 4324-4327, 2015. [CrossRef] [Google Scholar] [Publisher Link]

[5] Isabel Schlangen, and Alexander Charlish, "Distinguishing Small Targets from Sea Clutter Using Dynamic Models," *2019 IEEE Radar Conference (RadarConf)*, Boston, MA, USA, pp. 1-6, 2019. [CrossRef] [Google Scholar] [Publisher Link]

[6] Armin Parsa, and Noah H. Hansen, "Comparison of Vertically and Horizontally Polarized Radar Antennas for Target Detection in Sea Clutter — An Experimental Study," *2012 IEEE Radar Conference*, Atlanta, GA, USA, pp. 653-658, 2012. [CrossRef] [Google Scholar] [Publisher Link]

[7] M. Martorella, F. Berizzi, and E.D. Mese, "On the Fractal Dimension of Sea Surface Backscattered Signal at Low Grazing Angle," *IEEE Transactions on Antennas and Propagation*, vol. 52, no. 5, pp. 1193-1204, 2004. [CrossRef] [Google Scholar] [Publisher Link]

[8] Yong Yang, Shun-Ping Xiao, and Xue-Song Wang, "Radar Detection of Small Target in Sea Clutter Using Orthogonal Projection," *IEEE Geoscience and Remote Sensing Letters*, vol. 16, no. 3, pp. 382-386, 2019. [CrossRef] [Google Scholar] [Publisher Link]

[9] Junzhao Du et al., "Understanding Sensor Data Using Deep Learning Methods on Resource-Constrained Edge Devices," *11th China Wireless Sensor Network Conference*, Tianjin, China, pp. 139-152, 2018. [CrossRef] [Google Scholar] [Publisher Link]

[10] S. Panagopoulos, and J.J. Soraghan, "Small-Target Detection in Sea Clutter," *IEEE Transactions on Geoscience and Remote Sensing*, vol. 42, no. 7, pp. 1355-1361, 2004. [CrossRef] [Google Scholar] [Publisher Link]

[11] Jing Hu, Wen-Wen Tung, and Jianbo Gao, "Detection of Low Observable Targets within Sea Clutter by Structure Function Based Multifractal Analysis," *IEEE Transactions on Antennas and Propagation*, vol. 54, no. 1, pp. 136-143, 2006. [CrossRef] [Google Scholar] [Publisher Link]

[12] Dan Song et al., "Heavy-Tailed Sea Clutter Modeling for Shore-Based Radar Detection," *2018 IEEE Radar Conference (RadarConf18)*, Oklahoma City, OK, USA, pp. 1504-1509, 2018. [CrossRef] [Google Scholar] [Publisher Link]

[13] Pål Wessel, and Walter H.F. Smith, "A Global, Self-Consistent, Hierarchical, High-Resolution Shoreline Database," *Journal of Geophysical Research: Solid Earth*, vol. 101, no. B4, pp. 8741-8743, 1996. [CrossRef] [Google Scholar] [Publisher Link]

[14] M. Sciotti, and P. Lombardo, "Performance Evaluation of Radar Detection Schemes Based on CA-CFAR against K-Distributed Clutter," *2001 CIE International Conference on Radar Proceedings (Cat No.01TH8559)*, Beijing, China, pp. 345-349, 2001. [CrossRef] [Google Scholar] [Publisher Link]

[15] Alan G. Bole, Alan D. Wall, and Andy Norris, *Radar and Arpa Manual*, Elsevier Science, pp. 1-432, 1992. [Publisher Link]

[16] Jose C. Nieto-Borge et al., "Moving Ship Detection in Presence of Sea Clutter from Temporal Sequences of Marine Radar Images," *2008 International Conference on Radar*, Adelaide, SA, Australia, pp. 88-93, 2008. [CrossRef] [Google Scholar] [Publisher Link]